Supporting Information

Salt-Flower-Shaped FeP-CoP Catalyst for Highly Efficient Bifunctional Hydrogen and Oxygen Evolution

Ze-Feng Xu, Jia Xue, Lei-Lei Li*, Xing-Liang Yin*, Chuan-Wu Chen, Ya-Nan Jing, Da-Qiang Liu

Shandong Provincial Key Laboratory of Chemical Energy Storage and Novel Cell Technology, School of Chemistry and Chemical Engineering, Liaocheng University, Liaocheng, 252059, PR China

*Corresponding author E-mail: 88lileilei@163.com; xingliangyin@126.com

Experimental

1. Characterizations

The crystalline structures of the samples were determined by X-ray diffraction (XRD, SmartLab 9kW) using Cu Kα radiation. Morphologies and lattice structural information of the as-prepared samples were observed by scanning electron microscopy (SEM, Thermo Fisher Scientific FIB-SEM GX4) and transmission electron microscopy (TEM, Thermo Fisher F200x) with energy dispersive spectrometer (EDS) mapping. The surface chemical composition was analyzed by X-ray photoelectron spectroscopy (XPS, Thermo fisher Escalab Xi^+). The Brunauer-Emmett-Teller (BET) surface area was conducted by using an accelerated surface area and porosimeter system (Micromeritics ASAP-2460).

2. Electrochemical measurements

All electrochemical measurements were performed in a three-electrode system using an electrochemical workstation (Gamry Reference 3000). 3.20 mg of the as-synthesized catalysts was dispersed into 0.50 mL of mixture solution containing 20 μL Nafion and 480 μL isopropanol, and sonicated for 1 h to obtain a homogeneous ink. The glassy carbon electrode (GCE, 0.196 cm^2) loaded with 10 μL catalyst was used as the working electrode in 0.5 M H_2SO_4 solution (pH 1) for HER and 1.0 M KOH solution (pH 14) for OER. Hg/HgO and Hg/Hg_2SO_4 electrodes were choose as the reference electrodes for HER and OER, respectively. And a carbon rod was used as counter electrode. For HER and OER, linear sweep voltammetry (LSV) was measured at a scan rate of 5 mV/s from -1.8 V to -0.6 V and -0.1 V to 1.0 V, respectively. The electrochemical impedance spectroscopy (EIS) was obtained at the frequency range from 10^5 Hz to 10^{-2} Hz. The Cyclic Voltammetry (CV) at various scan rates (20, 40, 60, 80, 100, and 120 mV/s) were collected from -0.7 to -0.6 V for HER and 0.3 V to 0.4 V for OER. The stability was determined using the cyclic voltammetry and chronopotentiometric measurement. All potentials reported in this paper are referenced to reversible hydrogen electrode (RHE) with *iR* correction. All the above experiments were carried out in triplicate. In this study, the potentials were converted to RHE scales

using the following relationships: E (vs. RHE) = E (Hg/HgO) + 0.059 pH + 0.098; E (vs. RHE) = E (Hg/Hg_2SO_4) + 0.059 pH + 0.098. According to Tafel equation (formular 2): $\eta = b\log[j] + a$ to calculate the Tafel slope, where η is the overpotential, j is the current density, and b is the Tafel slope.

3. Turnover frequency calculations[1]

Cyclic voltammetry (CV) curves were recorded at a scan rate of 0.05 V s^{-1} in a phosphate buffered saline solution (1.0 M PBS, pH = 7.0). The number of active species (N) was determined using the following formula:

$$N = \frac{Q}{2F} = \frac{j \cdot t}{2F} = \frac{j \cdot V/u}{2F}$$

where Q is the cyclic voltammetric charge capacity obtained by integrating the CV cures, F is the Faradic constant (96485 C mol^{-1}), j is the current density (A), V is the voltage (V) and u is the scanning rate (V s^{-1}).

The TOF values are calculated via the following equation:

$$TOF = \frac{|j| \cdot A}{m \cdot F \cdot N}$$

In the context of a LSV measurement in a 1.0 M solution, the "|j|" denotes the absolute value of current density measured at a constant voltage. The "A" corresponds to the surface area of the electrode. Additionally, "F" refers to the Faraday constant. The "N" signifies number of active species for the electrochemical reactions. To account for the stoichiometry of the reactions involving water, a factor of 1/m is incorporated into the equation. This factor means the production of one H_2 or O_2 molecule from water requires the consumption of "m" electrons. Specifically, the hydrogen evolution reaction involves the transfer of 2 electrons, while the oxygen evolution reaction necessitates the participation of 4 electrons.

4. Determination of Faraday efficiency[2]

To validate the Faraday efficiency of FeP-CoP, an experiment was conducted

coupling a gas-tight electrochemical cell with a gas tube. An inverted graded measuring cylinders was employed to collect the escaping O_2 and H_2 gases. At an applied current density of 100 $mA \cdot cm^{-2}$, the experimental yields of H_2 and O_2 produced over 30 minutes were compared with theoretical predictions. The equation of Faraday efficiency is as follows:

$$\text{Faraday efficiency} = \frac{V_{\text{experimental}}}{V_{\text{theoretical}}} = \frac{V_{\text{experimental}}}{\frac{1}{n} \times \frac{Q}{F} \times V_m}$$

where Q is the charge passed through the electrode, F is Faraday constant (96485 $C \cdot mol^{-1}$), n represents that n moles of electrons are required for the production of each mole of H_2/O_2, V_m is the molar volume of gas (22.4 $L \cdot mol^{-1}$, 298 K, 101 KPa).

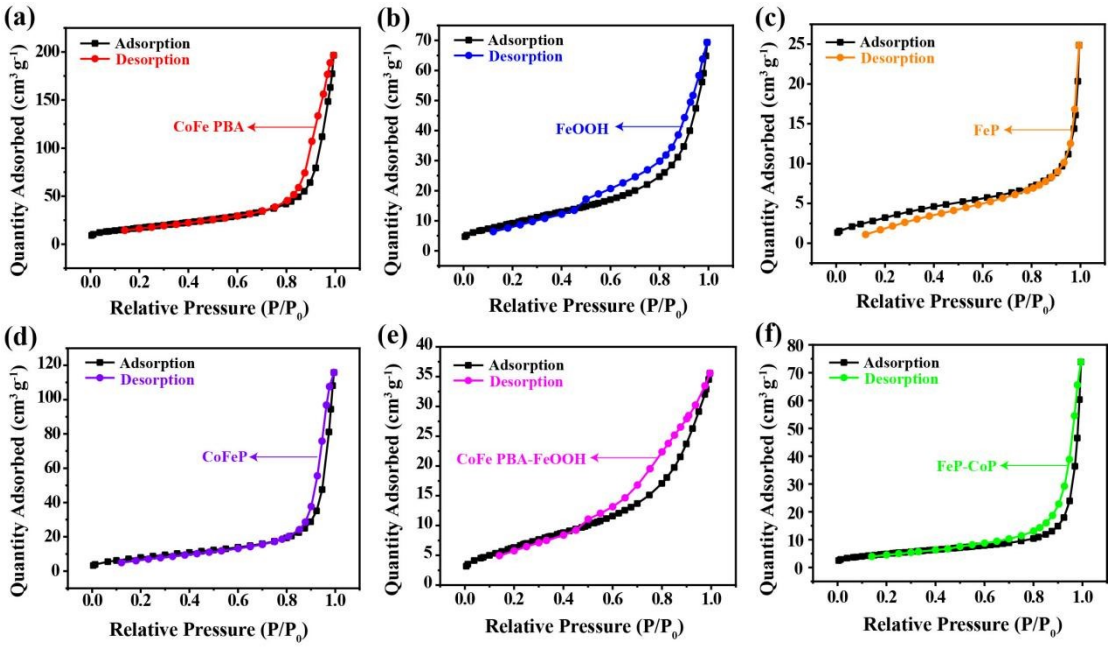

77

78 **Fig. S1.** Nitrogen adsorption-desorption isotherms of (a) CoFe PBA, (b) FeOOH, (c) FeP, (d)
79 CoFeP, (e) CoFe PBA-FeOOH, and (f) FeP-CoP.

80

81

82

83

84

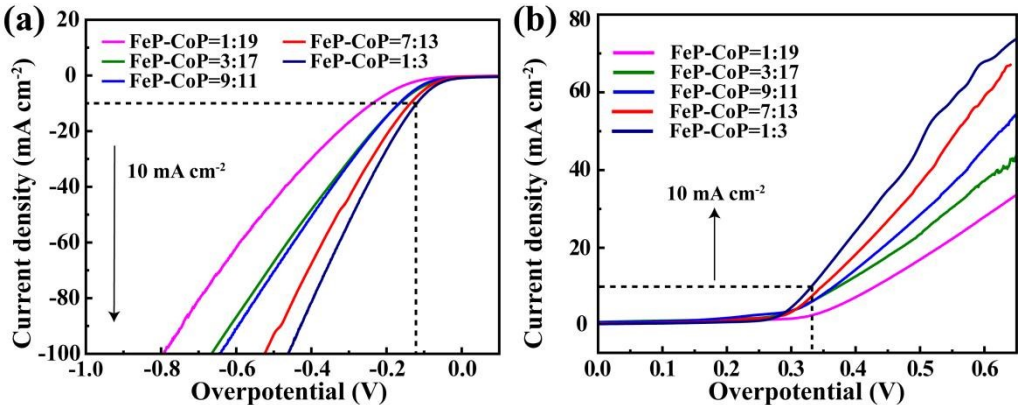

85

86 **Fig. S2.** (a) HER and (b) OER activities of FeP-CoP at different additional amounts of $FeCl_3$ in 0.5
87 M H_2SO_4 and 1.0 M KOH electrolytes, respectively.

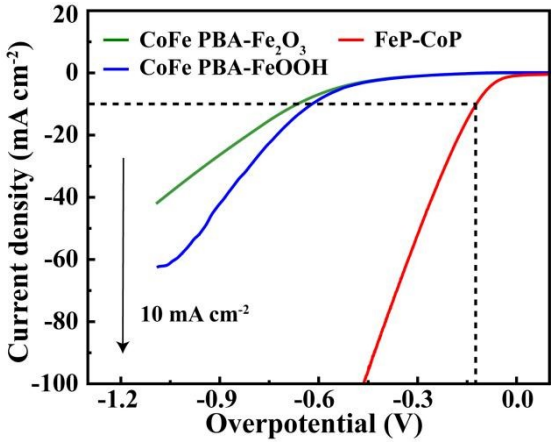

Fig. S3. The LSV curves of CoFe PBA-Fe_2O_3, CoFe PBA-FeOOH, and FeP-CoP in 0.5 M H_2SO_4.

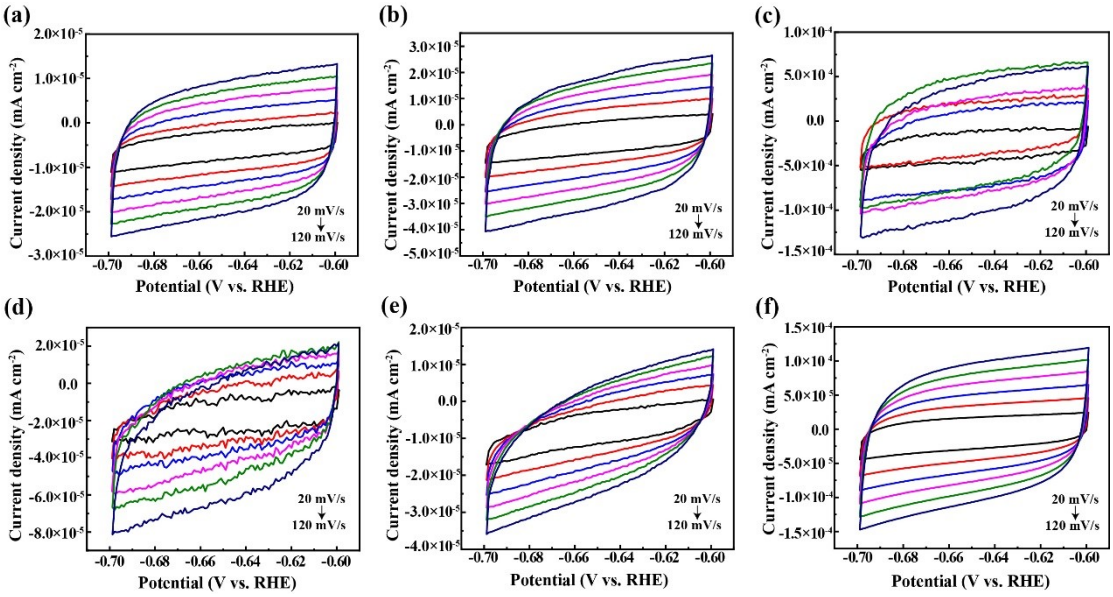

Fig. S4. (a) Electrochemical cyclic voltammograms of (a) CoFe PBA, (b) FeOOH, (c) FeP, (d) CoFeP, (e) CoFe PBA-FeOOH, and (f) FeP-CoP measured at different scan rates from 20 to 120 mV/s.

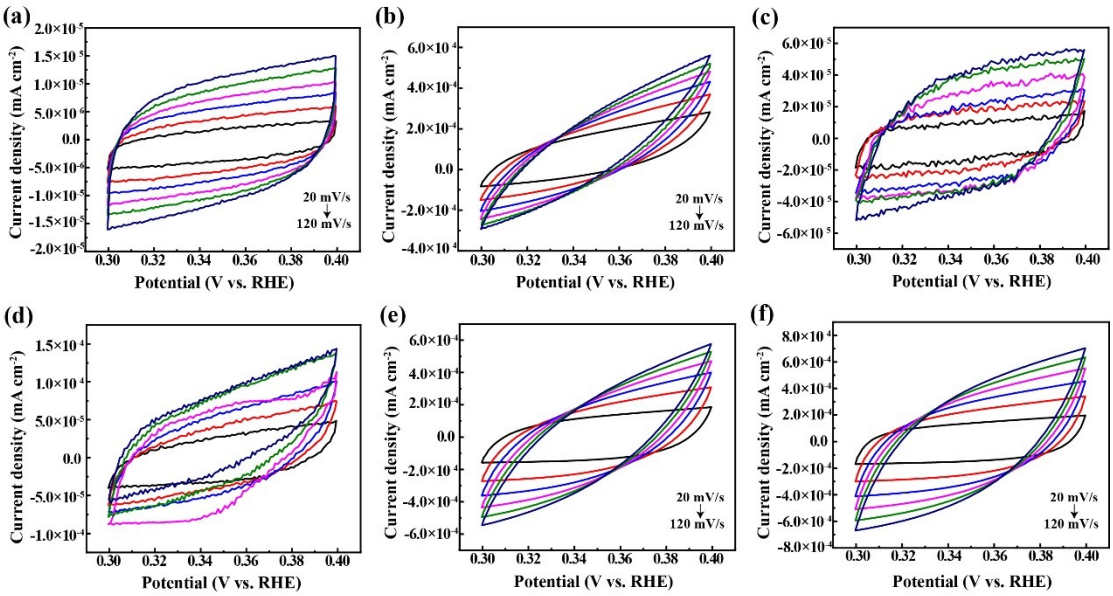

Fig. S5 (a) Electrochemical cyclic voltammograms of (a) CoFe PBA, (b) FeOOH, (c) FeP, (d) CoFeP, (e) CoFe PBA-FeOOH, and (f) FeP-CoP measured at different scan rates from 20 to 120 mV/s.

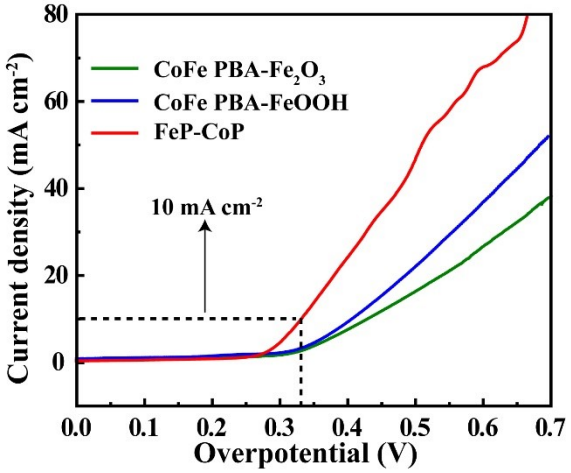

Fig. S6. The LSV curves of CoFe PBA-Fe_2O_3, CoFe PBA-FeOOH, and FeP-CoP in 1.0 M KOH.

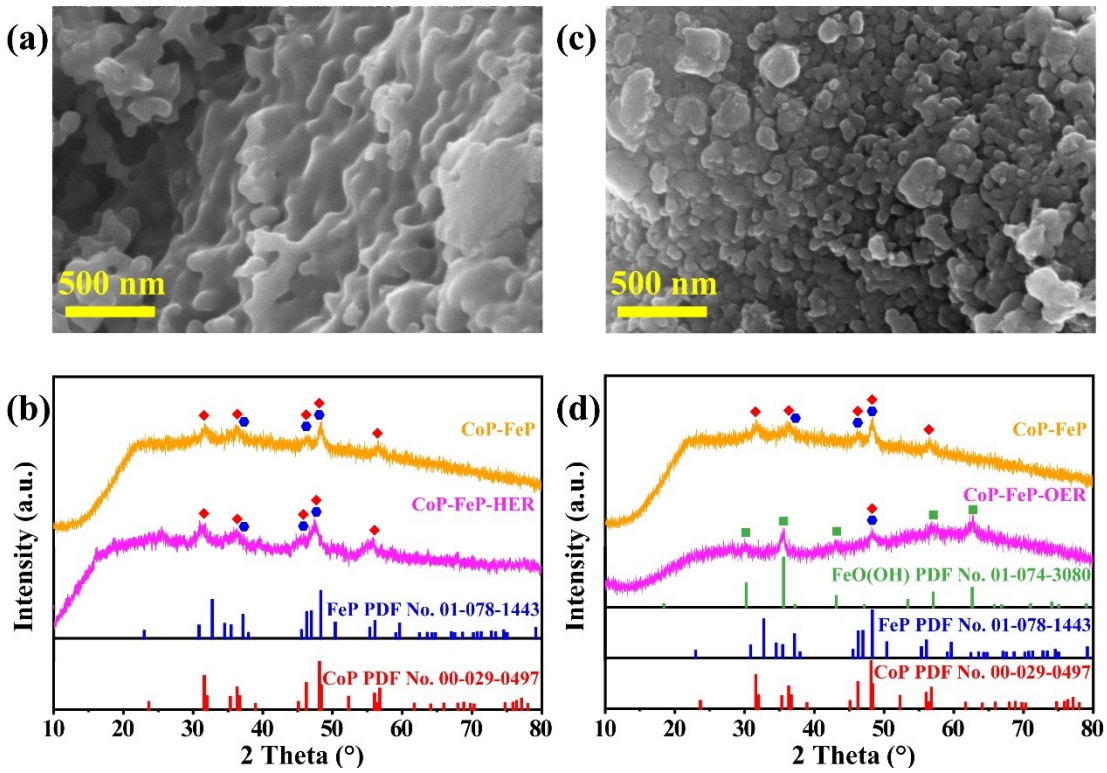

Fig. S7. (a) SEM image and (b) XRD pattern of FeP-CoP after HER stability test.(c) SEM image and (d) XRD pattern of FeP-CoP after OER stability test.

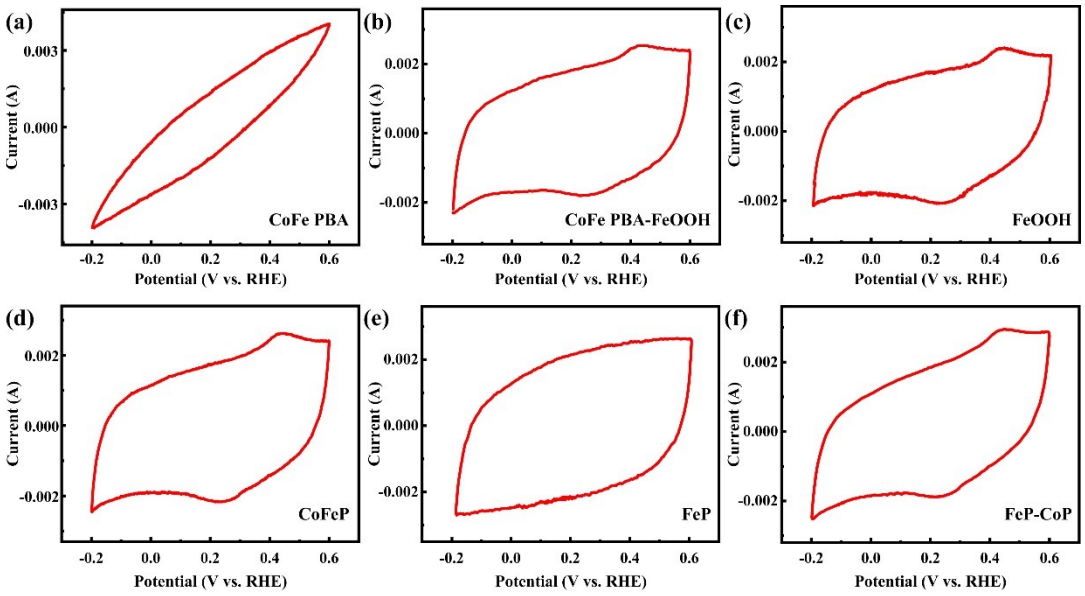

Fig. S8. CV curves at scan rates of 0.05 $V \cdot s^{-1}$ for the synthesized (a) CoFe PBA, (b) CoFe PBA-FeOOH, (c) FeOOH, (d) CoFeP, (e) FeP, and (f) FeP-CoP in 1.0 M PBS solution (pH = 7.0).

Table. S1. comparison of the HER and OER performances of FeP-CoP with those of other reported state-of-the-art non-precious metal-based electrocatalysts.

Catalysts	η^{10}_{HER} (mV)[a)]	Tafel slope (mV dec^{-1})[a)]	η^{10}_{OER} (mV)[b)]	Tafel slope (mV dec^{-1})[b)]	Reference
FeP-CoP	**105**	**106.73**	**320**	**93.27**	**This work**
Ni_2P/Fe_2P@NPC	155.3	78.55	237.8	111.68	[3]
FeMo@CoNi–OH/Ni_3S_2	177	89.3	160	73.5	[4]
$CoBO_x$/NiSe	107	153.4	229.1	11.7	[5]
Fe,Ni-$Co_{5.47}N$@N-rGO	124	58	234	171	[6]
NiCu-MoS_2	76	44	290	59	[7]
CMC/MC@C	102	89.43	336	81.71	[8]

a) Electrocatalysts in 0.5 M H_2SO_4 electrolyte.
b) Electrocatalysts in 1.0 M KOH electrolyte.
c) Stability test conducted at a current density of 10 mA cm^{-2}.

References

[1] Y. Shi, S. Zhou, J. Liu, X. Zhang, J. Yin, T. Zhan, Y. Yang, G. Li, J. Lai, L. Wang, An integrated amorphous cobalt phosphoselenide electrocatalyst with high mass activity boosts alkaline overall water splitting, Appl. Catal. B Environ. Energy, **341** (2024) 123326.

[2] M. D. Albaqami, M. U. Nisa, S. Mohammad, J. Hussain Shah, A. U. Rehman Baloch, A. G. Abid, S. Saleem, Phosphorus-doped $CuMn_2O_4$ nanoflakes: A highly performed electrocatalyst for oxygen evolution reaction and hydrogen evolution reaction in an alkaline environment, Energy & Fuels, **38** (2024) 15533-15542.

[3] D. I. Jeong, H. W. Choi, J. Kim, U. Y. Lee, B. K. Koo, B. K. Kang, D. H. Yoon, Ni_2P/Fe_2P encapsulated in N, P co-doped carbon shell as overall water splitting catalyst for wide pH range electrochemical applications, *Appl. Surf. Sci.*, **614** (2023) 156189.

[4] W. Fang, Y. Wu, S. Xin, Y. Hu, J. Dang, M. Li, B. Chen, H. Zhao, Z. Li, Fe and Mo dual-site single-atom catalysts for high-efficiency wide-pH hydrogen evolution and alkaline overall water splitting, *Chem. Eng. J.*, **468** (2023) 143605.

[5] Y. Liu, T. Sakthivel, F. Hu, Y. Tian, D. Wu, E.H. Ang, H. Liu, S. Guo, S. Peng, Z. Dai, Enhancing the d/p-band center proximity with amorphous-crystalline interface coupling for boosted pH-robust water electrolysis, *Adv. Energy Mater.*, **13** (2023) 2203797.

[6] Y. Kong, K. Guo, R. Liu, B. Yan, F. Shaik, B. Jiang, Fe/Ni-doped $Co_{5.47}N$ nanoparticles integrated on nitrogen-doped vertical reduced graphene oxide arrays for overall water splitting in wide pH range, *J. Electrochem. Soc.*, **170** (2023) 1945-7111.

[7] M. Kumar, T. C. Nagaiah, A NiCu–MoS_2 electrocatalyst for pH-universal hydrogen evolution reaction and Zn–air batteries driven self-power water splitting, *J. Mater. Chem. A*, **11** (2023) 18336-18348.

[8] S. Meng, H. Mao, W. Yaseen, M. Ji, Y. Xu, J. Xie, M. Xie, Facile synthesis of hierarchically ordered Mo_2C/Co_3Mo_3C@C nanosheet heterostructure: A highly durable pH universal electrocatalyst for hydrogen evolution reaction and overall alkaline water splitting, *J. Alloy. Compd.*, **969** (2023) 172440.